Original Article

The bioelectrical basis and validity of gastrointestinal extracellular slow wave recordings

Running Title

Bioelectrical basis of GI extracellular recordings

Authors and Affiliations

Timothy R. Angeli[1,2], Peng Du[1], Niranchan Paskaranandavadivel[1], Patrick W.M. Janssen[3], Arthur Beyder[4], Roger G. Lentle[2,3], Ian P. Bissett[5], Leo K. Cheng[1,6], Gregory O'Grady[1,5]

1. Auckland Bioengineering Institute, The University of Auckland, Auckland, New Zealand
2. Riddet Institute, Palmerston North, New Zealand
3. Institute of Food, Nutrition, and Human Health, Massey University, Palmerston North, New Zealand
4. Mayo Clinic, Rochester, Minnesota, USA
5. Department of Surgery, The University of Auckland, Auckland, New Zealand
6. Department of Surgery, Vanderbilt University, Nashville, Tennessee, USA

Corresponding Author

Gregory O'Grady

Auckland Bioengineering Institute, Private Bag 92019, Auckland 1142, New Zealand

Phone: +64 9 373 7599; Fax: +64 9 367 7157; email: ogrady.greg@gmail.com

Key Words

Gastric electrical activity, monophasic potential, motion artifacts, suction electrode

Total Word Count: 4588

Key Points

- Extracellular recording techniques are commonly used to measure bioelectrical activity. However, the validity of gastrointestinal extracellular recordings has recently been challenged.
- In this joint experimental and modelling study, slow waves were recorded during contractile inhibition, biphasic and monophasic slow wave potentials were recorded simultaneously, and the biophysical basis of extracellular potentials was modelled with comparison to experimental data.
- The results showed that *in-vivo* extracellular techniques reliably recorded slow waves in the absence of contractions, and potentials recorded using conventional serosal electrodes (biphasic) were concordant in phase and morphology with those recorded using suction electrodes (monophasic).
- Modelling further demonstrated that the morphology of experimental recordings is consistent with the biophysics underlying slow wave depolarisation.
- In total, these results demonstrate that gastrointestinal extracellular recordings are valid when performed and analysed correctly, reliably representing bioelectrical slow wave events. Motion suppression is not routinely required for *in-vivo* extracellular studies.

Word count: 150

Abstract

Gastrointestinal extracellular recordings have been a core technique in motility research for a century. However, the bioelectrical basis of extracellular data has recently been challenged by claims that these techniques preferentially assay movement artifacts, cannot reproduce the underlying slow wave kinetics, and misrepresent the true slow wave frequency. These claims motivated this joint experimental-theoretical study, which aimed to define the sources and validity of extracellular potentials. *In-vivo* extracellular recordings and video capture were performed in the porcine jejunum, before and after intra-arterial nifedipine administration. Gastric extracellular recordings were recorded simultaneously using conventional serosal contact and suction electrodes, and biphasic and monophasic extracellular potentials were simulated in a biophysical model. Contractions were abolished by nifedipine, but extracellular slow waves persisted, with unchanged amplitude, downstroke rate, velocity, and downstroke width ($p>0.10$ for all), at reduced frequency (24% lower; $p=0.03$). Simultaneous suction and conventional serosal extracellular recordings were identical in phase (frequency and activation-recovery interval), but varied in morphology (monophasic vs. biphasic; downstroke rate and amplitude: $p<0.0001$). Simulations demonstrated the field contribution of current flow to extracellular potential and quantified the effects of localised depolarisation due to suction pressure on extracellular potential morphology. In sum, these results demonstrate that gastrointestinal extracellular slow wave recordings cannot be explained by motion artifacts, and are of a bioelectrical origin that is highly consistent with the underlying biophysics of slow wave propagation. Motion suppression is shown to be unnecessary as a routine control in *in-vivo* extracellular studies, supporting the validity of the extant gastrointestinal extracellular literature.

Abbreviations

GI: Gastrointestinal

FEVT: Falling-edge, variable-threshold

ICC: Interstitial cells of Cajal

PCB: Printed circuit board

SNR: Signal-to-noise ratio

cpm: cycles per minute

Introduction

Extracellular recordings taken directly from the surface of the gastrointestinal (GI) tract have been a core technique in motility research for a century. In classic studies, Alvarez and colleagues recorded extracellular potentials from the stomach and small intestine, first demonstrating the concordance between slow wave and contraction frequencies (Alvarez & Mahoney, 1922),(Berkson *et al.*, 1932).

In the normal human stomach *in-vivo*, extracellular recordings have shown that the slow wave frequency is ~3 cycles min^{-1} (cpm), with the distal stomach being entrained to a pacemaker on the greater curvature of the corpus (Hinder & Kelly, 1977),(O'Grady *et al.*, 2010). Extracellular recordings have further demonstrated that this slow wave entrainment is underpinned by a declining intrinsic frequency gradient from corpus to antrum, such that distal areas autonomously activate at a lower frequency if isolated (Kelly & Code, 1971),(Sarna *et al.*, 1972*a*),(Hinder & Kelly, 1977). These descriptions underpin clinical interpretations of cutaneous electrogastrography (Yin & Chen, 2013).

Recently, however, the validity and biophysical basis of GI extracellular recordings were critically challenged by two studies (Bayguinov *et al.*, 2011),(Rhee *et al.*, 2011). In one study, Bayguinov *et al.* reported that contraction artifacts could be recorded using extracellular electrodes in *in-vitro* murine gastric tissue strips (Bayguinov *et al.*, 2011). When these contractions were suppressed with nifedipine or wortmannin, the authors could not record extracellular slow wave activity, but they could record intracellular slow waves. They concluded that extracellular methods, in general, assay movement artifacts and not bioelectrical activity, and that controls for movement must accompany extracellular studies. Furthermore, based on theoretical notes, Bayguinov *et al*. argued that the slow wave voltage transients recorded by extracellular methods are inconsistent with the underlying kinetics of slow wave depolarisation and repolarisation.

In the second study, which was published in this journal, Rhee *et al*. performed intracellular recordings on isolated human gastric tissue strips, and reported that the human gastric slow wave frequency is actually 5-8 cpm, rather than the 3 cpm demonstrated in extracellular studies, and that there is no intrinsic human gastric frequency gradient (Rhee *et al.*, 2011). To explain why their data conflicted with previous extracellular studies, Rhee *et al*. claimed that GI extracellular recordings are generally invalid, because extracellular techniques cannot record authentic slow waves, instead recording motion artifacts that have underestimated the true frequency.

Extracellular GI recordings underpin a substantial and important motility literature (Szurszewski, 1998), and further investigations are now needed to clearly establish the sources and validity of extracellular data.

In the current study, we therefore aimed to determine whether *in-vivo* extracellular recording methods can reliably detect slow wave potentials in the absence of contractions. We further aimed to quantitatively define the relationship between extracellular slow wave morphologies and the biophysics of the underlying slow wave activation. We chose to restrict our focus to *in-vivo* methods in this work, because it is *in-vivo* extracellular recordings that primarily underpin relevant clinical methods and concepts. These aims were tested in a series of joint experimental-theoretical studies.

Methods

Animal Preparation

Ethical approval for the experiments was obtained from The University of Auckland Animal Ethics Committee. All experiments were performed *in-vivo*. The studies were performed on seven cross-breed weaner pigs of mean weight 31.7 ± 2.1 kg. These animals were subjected to an overnight fast, followed by general anaesthesia induced with Zoletil (Tiletamine HCl 50 mg mL^{-1} and Zolazepam HCl 50 mg mL^{-1}), and maintained with Isoflurane (2.5 - 5% with an oxygen flow of 400 mL within a closed-circuit anaesthetic system). Surgical access was by midline laparotomy. Vital signs including oxygen saturations, heart rate, blood pressure, and core temperature were continuously monitored and maintained within normal physiological limits. At the conclusion of the studies, the animals were euthanised with a bolus injection of 50 mL of a saturated solution of magnesium sulphate, while still under anaesthetic.

Extracellular Slow Wave Recordings

Small Intestine Recordings

The aim of these experiments (*n* = 5 pigs) was to record and compare GI extracellular potentials before and after the suppression of contractions *in-vivo*. Intestine recordings were chosen for this experiment because the amplitude and signal-to-noise ratio (SNR) of porcine intestinal extracellular slow wave events (40-140 μV) is much less than that of gastric events (800-1300 μV) (Angeli *et al.*, 2013*a*),(Egbuji *et al.*, 2010), thereby provide a more rigorous test for the detection of low amplitude electrical events in living tissues.

In each experiment, a short segment of jejunum (20-30 cm) was exteriorised and the terminal arterial branch from the superior mesenteric arcade supplying that segment was isolated and cannulated with a 23-gauge angiocatheter. A brief 0.9% saline flush was administered, causing temporary blanching to confirm that the exteriorised segment was

perfused by the cannulated artery. High-resolution extracellular slow wave recordings and motion capture video recordings (described below) were then performed in immediate succession before and after intra-arterial administration of nifedipine (80 μg kg^{-1} bolus, followed by 8 μg kg^{-1} min^{-1} infusion; a dosage estimated to be equivalent to 10 μM nifedipine). Nifedipine was obtained from Sigma-Aldrich (MO, USA).

Extracellular recordings were performed using high-resolution flexible printed circuit board (PCB) arrays with 0.3 mm gold contacts (128 electrodes; 4 mm inter-electrode spacing) attached to copper wires in a polyimide film (Du *et al.*, 2009). These arrays were housed in silicone cradles that conformed them in gentle contact with the serosa of the intestinal circumference (Angeli *et al.*, 2013*b*). Warm saline was applied at regular intervals to exteriorised intestinal loops to minimise serosal cooling and drying. Ventilation was paused for regular 30 s intervals during recordings to minimise respiratory artifacts.

Gastric Recordings

The aim of these experiments (*n* = 3 pigs) was to record and compare morphologies of slow wave potentials using two methods of extracellular recordings: suction electrodes and conventional serosal contact electrodes. These recordings were also applied to inform and validate the biophysical basis of the extracellular potential model described below. Suction electrodes have been widely used in electrophysiology to record monophasic action potentials, representing the time course of the action potential over many cells (Franz, 1999), including in GI electrophysiology studies (e.g., (Bozler, 1945),(Bortoff, 1967)).

The suction electrode was of standard silver-wire glass-pipette construction (#573000, A-M Systems, WA, USA). The capillary tube (diameter 1.2 mm) was filled with saline solution, the electrode was lowered onto the serosa, and gentle suction pressure was applied until a portion of the serosa invaginated into the capillary (Figure 1c). The electrode was held in position by a test-tube clamp set. The conventional serosal contact electrodes were the same PCB arrays described above (Figure 1c). These arrays were placed over the gastric

serosa and gently held in contact with aid of warm saline-soaked gauze packs. Both electrode types were applied simultaneously *in-vivo* on directly-adjacent regions of the anterior porcine gastric serosa, near the mid-corpus of the greater curvature (Figure 1a). These experimental manipulations were performed with minimal gastric handling and the laparotomy wound was then approximated and covered with warm saline-soaked gauze to maintain the normal serosal temperature and moisture. As above, ventilation was paused for 30 s intervals.

Data Acquisition and Analysis

Extracellular recordings were performed using an ActiveTwo System (BioSemi, The Netherlands) that was modified for passive recordings, with customised acquisition software in LabView (National Instruments, TX, USA), and with reference electrodes placed on the hindquarter thigh (Egbuji *et al.*, 2010). Recordings were performed at 512 Hz, downsampled to 30 Hz, and filtered with a moving median filter to remove baseline drift and a Savitzky-Golay filter to remove high-frequency noise (effective low-pass cut-off ~2 Hz). These filters have been validated as optimal for *in-vivo* extracellular slow wave recordings (Paskaranandavadivel *et al.*, 2013).

Electrical analyses were performed in Matlab v7.9 (Natick, MA, USA) using the Gastrointestinal Electrical Mapping Suite (GEMS) v1.5 (Yassi *et al.*, 2012). For PCB electrode recordings, slow wave activation times were identified using the validated FEVT algorithm (Erickson *et al.*, 2010),(Angeli *et al.*, 2013*b*), followed by manual review. FEVT identifies activation times as the point of maximum downstroke rate using a signal transform with a variable threshold approach to detect the slow wave downstrokes. Recovery times were next detected as the point of maximum upstroke after the activation time, using a low-pass derivative Savitzky Golay algorithm (polynomial order: 5, window width: 2 seconds) (Savitzky & Golay, 1964). Slow wave activation maps, frequency, amplitude, and velocity were calculated using validated automated methods (Paskaranandavadivel *et al.*,

2011),(Paskaranandavadivel *et al.*, 2012),(Yassi *et al.*, 2012). Slow wave downstroke rate was calculated as the derivative of the signal at the activation time, and downstroke width was calculated as the time difference between the peak and trough of the slow wave deflection.

The FEVT algorithm was not designed to analyse monophasic action potentials, so an alternative method was developed to analyse the suction electrode recordings. Following filtering, a second-order non-linear energy squared operator was applied (Kaiser, 1990), followed by a moving variable threshold to identify the points representing slow wave events. These points were then identified as the point of maximum upstroke or downstroke of the monophasic slow wave event using Savitzky Golay derivatives (polynomial order 9; window 2 s) (Savitzky & Golay, 1964).

Video Recording and Contraction Analysis

Video was captured using a high-definition Sony NEX-VG10 video camera (Tokyo, Japan). The video was converted to still images and analysed at a rate of five frames per second with a line of interest (LOI) placed through the region of the isolated intestinal segment that was perfused by the cannulated arterial branch. Maps of longitudinal strain rate ('L maps') were created based on the LOI, using a custom analysis program, by the methods of Janssen *et al.* (Janssen *et al.*, 2009). The longitudinal distribution of strain rate indicated regions of contraction and relaxation in the L maps, with single-pixel-level (sub-millimetre) resolution (Lentle *et al.*, 2012). Contractile presence was compared before and after administration of nifedipine.

Statistical Comparisons

Slow wave characteristics for the intestinal experiments were compared using a general linear model in SAS v9.2 (SAS Institute Inc., NC, USA). Gastric slow wave comparisons between PCB and suction electrodes were performed using Student's t-test (unpaired, equal

variance). Means ± SEMs or SDs are reported, as appropriate, and the significance threshold was $p < 0.05$.

Extracellular Slow Wave Potential Model

The aim of this experiment was to define the biophysical basis of extracellular slow wave potentials, and then to compare theoretical and experimental results. The basis of extracellular potential (ϕ_e) in relation to membrane potential was investigated using a core-conductor mathematical model, which was based on the extracellular models proposed by Spach *et al.* and Barr, and a slow wave cell model proposed by Imtiaz *et al.* (Spach *et al.*, 1972),(Barr, 2000),(Imtiaz *et al.*, 2002). A bundle of muscle fibres was modelled as a cylinder, with radius (a) and length (L), as illustrated in Figure 2. The intracellular tissue conductivity was denoted by σ_i and the extracellular conductivity tissue was denoted by σ_e. The membrane current due to conduction of slow waves (I_m) was assumed only to vary along the length of the model, resulting in the following equation used to calculate the distribution of ϕ_e in the polar-coordinate form (Barr, 2000),

$$\phi_e(r', x') = \frac{1}{4\pi\sigma_e}\int_0^L \frac{I_m(x)}{\sqrt{r'^2+(x-x')^2}}dx \qquad \text{(Eqn. 1)}$$

where I_m can be expressed as a function of membrane potential (V_m),

$$I_m(x) = \pi a^2 \sigma_i \frac{\partial^2 V_m}{\partial x^2} \qquad \text{(Eqn. 2)}$$

The variance of V_m in both the distance along the cylindrical model as well as in time was represented in the partial derivative.

The dimensions of the cylindrical model were a = 0.25 mm and L = 9 mm (VanHelden & Imtiaz, 2003). Slow wave propagation was simulated along the model, at a velocity of 8.0 mm s^{-1} that is consistent with porcine gastric activation (Egbuji *et al.*, 2010), to calculate I_m and ϕ_e using the above equations. To simulate monophasic extracellular potentials, a 1.2 mm section of the middle region of the model was voltage-clamped to -32 mV, which

presented the localised depolarising effect of suction on the tissue, as previously reported in cardiac tissue (Franz, 1999). The ratio of σ_i / σ_e was also reduced to one-third that of the value used for the biphasic model, to simulate the effect of pressure causing diffusion of fluid into the extracellular matrix (Tranquillo *et al.*, 2004). The I_m was sampled at four points along the length of the fibre, as shown in Figure 2. The two middle points were chosen to be directly adjacent to the electrode contact and were different for the conventional serosal contact and suction electrode because of the different contact diameters (0.3 versus 1.2 mm). The simulated extracellular potentials were compared to the simulated membrane potential, V_m.

Results

Intestinal Extracellular Recordings and Motion Suppression

Spatiotemporal video analysis revealed that 4/5 pigs demonstrated contractile activity prior to the administration of nifedipine (Figure 3a). Under these *in-vivo* experimental conditions, the contractile patterns were variable and inconsistent between subjects, in accordance with the known consequences of the surgical methods (e.g., (Alvarez & Mahoney, 1922)). One animal displayed widespread static (non-propagating) contractions (Figure 3a), three animals displayed intermittent static contractions, and one animal displayed no baseline contractile activity. In all cases, all contractile activity was successfully blocked by nifedipine, with complete abolition of all contractile activity observed in the high-definition video analysis of all animals after the administration of nifedipine (Figure 3b).

Slow waves were consistently identified before and after the administration of nifedipine in all 5 pigs (Figure 3c,d). Electrical analysis comprised approximately 7500 identified slow wave events (3300 before nifedipine; 4200 after nifedipine and contraction suppression). Average slow wave amplitude, velocity, downstroke width, and downstroke rate remained similar between pre-nifedipine and post-nifedipine recordings, while average slow wave frequency decreased by 24% ($p = 0.03$) (Table 1).

Gastric Extracellular Slow Wave Morphologies

Comparison of suction and conventional extracellular potential morphologies were performed on conventional serosal contact electrodes directly adjacent to the suction electrode. The two types of gastric extracellular recording methods demonstrated substantially different morphologies: the suction electrode recorded monophasic extracellular potentials (Figure 4a), while the conventional serosal contact electrodes recorded biphasic extracellular potentials (Figure 4d). The two signal morphologies, which were recorded simultaneously, matched in frequency and duration but displayed morphological differences, as quantified for amplitude and downstroke rate in Table 2. The activation-recovery intervals

of the two signal morphologies were comparable, as demonstrated in Table 2, showing that recovery potentials could be accurately identified in the conventional serosal contact electrode recordings.

Extracellular recordings are generally known to approximate intracellular recordings by their second derivative (e.g., (Cohen & Miles, 2000),(Spach *et al.*, 1979)). This relationship was evaluated here for the two types of gastric extracellular methods, with suction electrodes approximating intracellular recordings (Shabetai *et al.*, 1968),(Hoffman *et al.*, 1959), as a method of comparing and cross-validating the two extracellular slow wave recording methods. The first and second derivatives of the monophasic signals recorded by the suction electrode were calculated and a 20 point moving average filter was applied to remove noise amplification (Figure 4b and 4d). Comparable waveform morphology was observed between the biphasic conventional serosal contact electrode recording (Figure 4d) and the second derivative of the monophasic suction electrode recording (Figure 4c).

Extracellular Slow Wave Potential Model

To evaluate the timing and morphological correlations between membrane and extracellular potentials, a single event of the simulated V_m at the middle of the fibre (x = 4.5 mm) was compared to the simulated ϕ_e at r = 2.66 mm radially away from the centre of the fibre. This value of r = 2.66 mm represents the thickness of gastric musculature between the electrode and fibre (Huh *et al.*, 2003). The simulated ϕ_e near the middle of the fibre demonstrated the typical biphasic morphology recorded using a conventional serosal contact electrode, with an initial positive phase followed by a rapid negative phase and then recovery to the baseline (Figure 5b). The timing of the activation point in the downstroke phase of the simulated ϕ_e also matched the timing of the downstroke of the simulated V_m at the same location (Figure 5a).

The biphasic shape of the simulated extracellular potential also closely matched the shape of the simulated I_m at four locations along the fibre (x = 1.5, 4.35, 4.65, and 7.5 mm; Figure

5c). However, the duration of the extracellular potential was longer than the duration of I_m (270 ms versus 230 ms), indicating that multiple I_m in a field contribute to the resultant ϕ_e.

A suction electrode extracellular recording was simulated by holding the V_m in the region under the electrode contact to -32 mV (Franz, 1999). With the region directly under the suction electrode contact held at a constant value (Figure 5d), the resultant extracellular potential morphology remained monophasic (Figure 5e). The baseline of the simulated monophasic potential was negative (-0.83 mV) and the peak potential was positive (0.47 mV), which matched the experimental observations (Figure 4).

Compared to the biphasic morphology, which alternates between positive and negative potentials as a result of a slow wave approaching and leaving an electrode (Barr, 2000), the depolarising effect of the suction electrode introduces additional currents to the tissue directly beneath the electrode and therefore alters the extracellular morphology (Franz, 1999). The effect of suction on the local tissue was further elucidated by studying the current flow in the model. The simulated I_m demonstrated variations in morphology, with the I_m close to the suction electrode contact, which was at the middle of the fibre (x = 4.5 mm), showing monophasic morphology (at x = 3.9 and 5.1 mm; from -100 to -19 mA mm^{-1}), and the I_m further away from the contact retaining biphasic morphology (at x = 1.5 and 7.5 mm). The amplitudes of the simulated monophasic I_m were also higher than the biphasic I_m further away from the location of contact (81 vs. 2 mA mm^{-1}), which correlated to a higher amplitude of monophasic potential (Franz, 1999),(Jochim *et al.*, 1935). The effect of suction pressure on I_m was limited to a very localised region in the model, as shown by the retention of the biphasic I_m morphology sampled at two points further away from the suction electrode contact (x = 1.5 and 7.5 mm) (Figure 5). The change in I_m required to reproduce the monophasic potential indicated that the suction pressure induced a physical change to the electrical field around the site of contact.

Discussion

This study has demonstrated that: i) extracellular recording techniques readily and reliably record intestinal slow waves *in-vivo* in the absence of contractile activity; ii) gastric extracellular slow wave potentials recorded using conventional serosal contact electrodes are concordant in phase and morphology with monophasic potentials recorded using suction electrodes, which approximate intracellular recordings; and iii) the morphology of conventional and suction extracellular recordings are consistent with the biophysics of the underlying slow wave depolarisation.

In sum, these results strongly support the validity of GI extracellular slow wave recordings. Our study therefore resolves current controversy and confusion in the field regarding whether extracellular data, including that derived from multi-electrode arrays, represents electrical events or motion artifacts (Bayguinov *et al.*, 2011),(Rhee *et al.*, 2011). It is conclusively shown that extracellular slow wave recordings are of true bioelectrical origin.

Our findings that slow waves persist in the absence of contractile activity contrast with those of Bayguinov *et al.*, who were unable to record extracellular potentials in murine stomach *in-vitro* after motion suppression (Bayguinov *et al.*, 2011). These differing results may be explained by methodological differences, including that pigs have higher slow wave amplitudes than mice, supporting their easier detection (Egbuji *et al.*, 2010),(Wang *et al.*, 2005). In addition, the filtering methods applied here are validated to be appropriate for slow wave detection, whereas the methods of Bayguinov *et al.* could have eliminated important slow wave content and accentuated artifacts (Paskaranandavadivel *et al.*, 2013). *In-vivo* recordings in living whole-organs may also be more readily achieved than *in-vitro* recordings in isolated tissue strips, because extracellular methods detect a cohesive propagating activation wave through tissues, which may be disrupted by the tissue devascularisation and dissection necessary for *in-vitro* preparations (Xue *et al.*, 1995). Lammers *et al.* have achieved *in-vitro* extracellular GI recordings in several species, showing slow wave

morphologies comparable to those reported here, but recommended specific adaptations to preserve tissue viability, *e.g.* high perfusion rates, customised arrays allowing perfusate flow between electrodes, and gentle contact (Lammers *et al.*, 1993),(Lammers *et al.*, 2002).

The claim by Bayguinov *et al.* that contractile inhibition is routinely required as a control for extracellular recordings (Bayguinov *et al.*, 2011), is not supported by our results, because motion suppression affected little change on extracellular slow waves *in-vivo*. This is particularly important, because contractile suppression would often be impractical *in-vivo*, especially in clinical studies. The only significant difference noted after administration of nifedipine was a reduction in frequency. The cause of this frequency change was not a focus of this work, but intracellular studies have previously shown that slow wave frequency is unaffected by nifedipine (Huang *et al.*, 1999),(Malysz *et al.*, 1995), suggesting that the frequency decrease observed in this study may have been a result of slight tissue cooling following the repeated evisceration for video mapping (El-Sharkawy & Daniel, 1975).

The *in-vivo* contractile patterns observed in this study were variable, and in one case, quiescent. It has long been known that contractile activity can be variable and suppressed under *in-vivo* open-abdomen experimental conditions, with Alvarez describing a “hush that seems to fall upon its contents" when the abdominal cavity was surgically entered, due to a sympathetically-mediated inhibition (Alvarez & Mahoney, 1922),(Bueno *et al.*, 1978). Early researchers therefore would sometimes pith the spinal cord in the region distal to the inter-scapular segment to study motility (Alvarez & Hosoi, 1929). Modern motility mapping studies have generally been carried out under controlled *in-vitro* conditions, where contractile patterns can be readily assessed (Hennig *et al.*, 1999),(Lammers *et al.*, 2001),(Lentle *et al.*, 2012). The relatively heightened contractility of *in-vitro* tissues may make artifacts more problematic when attempting extracellular recordings in that context, as investigated by Bayguinov *et al.* (Bayguinov *et al.*, 2011).

Our study supports the veracity of the GI extracellular recording literature, including fundamental descriptions of human gastric slow wave activation and intrinsic frequency gradients (Kelly & Code, 1971),(Hinder & Kelly, 1977),(O'Grady *et al.*, 2010). Importantly, however, results from these previous extracellular studies differ from recent intracellular data showing a human gastric slow wave frequency of 5-8 cpm, with no intrinsic frequency gradient (Rhee *et al.*, 2011). The most likely explanation for this disparity is that the process of tissue isolation and preparation required for intracellular recordings induces changes in slow wave frequencies and gradients (Suzuki *et al.*, 1986),(O'Grady *et al.*, 2012*c*). For example, Xue *et al.* found that slow wave frequencies became elevated and gradients were altered or lost following tissue dissection, with prostaglandin release being implicated (Xue *et al.*, 1995). Furthermore, the contraction frequency in isolated *in-vitro* human gastric tissues has also been reported to range from 4-5 cpm (Sinn *et al.*, 2010), compared to the 3 cpm activity shown to occur *in-vivo* by various methods, including MRI (Marciani, 2011),(Hocke *et al.*, 2009). It would be valuable if the mechanisms responsible for these effects were now fully elucidated to clarify past and future interpretations of *in-vitro* data.

Extracellular slow wave recordings are often of low amplitude and SNR, and the potential for movement and other artifacts to contaminate and distort extracellular signals is well known. Numerous other past investigators have therefore also critically questioned the bioelectrical origin of extracellular recordings, most coming to similar conclusions to this study, albeit by less rigorous approaches (e.g.(Berkson *et al.*, 1932),(Bozler, 1939),(Richter, 1924)). Beyond the results of our current study, the bioelectrical validity of extracellular slow wave recordings is further supported by observations that: extracellularly-recorded slow wave frequencies can be controlled by extrinsic pacing; the timing of the major negative deflection of the biphasic potential (*i.e.,* wavefront) precedes the contraction; and simultaneous extracellular recordings of slow waves and intestinal movements demonstrate characteristically different morphologies (O'Grady, 2012). In addition, the velocity of slow wave propagation and amplitudes of extracellular potentials are directly correlated, which can be explained by

bioelectrical mechanisms but not artifacts, whereby increased current enters the extracellular space when velocity increases (O'Grady *et al.*, 2012*b*).

In the present study, we elected to focus on *in-vivo* extracellular recordings because *in-vivo* techniques underpin relevant clinical investigations, including serosal mapping and cutaneous electrogastrography (Smout *et al.*, 1980),(O'Grady *et al.*, 2012*a*). Intracellular recordings were not performed, but suction electrodes could be effectively applied *in-vivo*. Monophasic potentials recorded by suction electrodes reflect intracellular potentials simultaneously occurring across many cells (Hoffman *et al.*, 1959), and our monophasic potential morphology matched well with published intracellular slow wave traces (e.g. (Dickens *et al.*, 1999)). The amplitude of the suction electrode recordings was much higher than that of the conventional serosal contact electrodes, because suction caused local membrane defects in the underlying tissue, decreasing the resistance between the electrode and source (Franz, 1983).

Suction recordings are also particularly useful for determining activation-recovery intervals (Coronel *et al.*, 2006),(Yue *et al.*, 2004), a property utilised here to demonstrate that conventional serosal contact methods reliably indicate both slow wave depolarisation and repolarisation currents. Extracellular slow wave mapping studies to date have typically focused only on mapping wavefronts, but repolarisation dynamics may also be critical in the initiation and maintenance of gastric dysrhythmia (O'Grady *et al.*, 2011). It would be interesting to now apply extracellular repolarisation mapping to investigate gastric dysrhythmia mechanisms, as is achieved in cardiac electrophysiology (e.g., (Yue *et al.*, 2004)).

The model presented in this study demonstrates that the morphology of extracellular potentials follows a field-effect of an electrical source away from the location of the electrode contact. In order to integrate the contributions of slow wave potentials over a fibre, the model assumed that the simulated slow wave travels within a volume conductor whereby currents

flow throughout the extracellular tissue space, diminishing in amplitude with distance away from the fibre, as previously described (Barr, 2000). Alternative cell models, such as the relaxation oscillator models, could also be used to simulate propagation of slow waves in the fibre, perhaps as a computationally efficient model to study the field contribution of a large area of tissue where the variability of slow waves is a factor (Sarna *et al.*, 1971),(Sarna *et al.*, 1972*b*); however, the trade-off is the potential loss of biophysical mechanisms of slow wave propagation and some details in the simulated slow wave morphology (Cheng *et al.*, 2010). The simulation results demonstrated that even though a field containing multiple electrical sources summates to generate an extracellular potential (De-Bakker & Wittkampf, 2010), the correlation between the downstroke of the biphasic extracellular potential and the upstroke of membrane potential in the immediate vicinity to the extracellular electrode was clear (Figures 5a and 5b). This close correlation could be explained by Eqn. 1, which demonstrates that as the source moves further away, the contribution of the source on the extracellular potential decreases hyperbolically. This means that only the closest membrane potentials contribute significantly to the summated extracellular potential. Furthermore, when the local tissue beneath the electrode was perturbed by the depolarising effect of suction, the potential difference compared to the surrounding tissue was proposed to lead to an 'injury current,' which changed the morphology of extracellular potential to a monophasic shape (Franz, 1999).

In conclusion, this joint experimental-theoretical study has demonstrated that extracellular electrical recordings represent true biopotentials that are consistent with the underlying biophysical properties of slow wave propagation, and are not contractile artifacts, as was recently claimed by others. This study supports and validates the gastrointestinal extracellular literature and demonstrates that contractile suppression is an unnecessary step for recordings carried out under comparable experimental and technical conditions.

Acknowledgements

We thank Linley Nisbet for her expert technical assistance.

Contributions

TRA, PD, GOG designed the study and wrote the manuscript. TRA led the intestinal studies; GOG, AB the gastric studies; PD the modelling studies; NP the morphology comparisons; and PWMJ, RGL the motion analysis. IPB and LKC provided critical intellectual input and supervision. All authors critically revised and approved the final manuscript. All experiments were performed at The University of Auckland, Auckland, New Zealand.

Funding

The work / authors were supported by funding from the New Zealand Health Research Council, the National Institute of Health (R01 DK64775), and the Riddet Institute. TRA was supported by the Riddet Institute Earle Food Research Scholarship and the Royal Society of New Zealand R.H.T. Bates Postgraduate Scholarship. PD is supported by the NZ Marsden Fund and a Rutherford Foundation New Zealand Postdoctoral Fellowship.

References

Alvarez WC & Hosoi K (1929). What has happened to the unobstructed bowel that fails to transport fluids & gas? *Am J Surg* **6,** 569–578.

Alvarez WC & Mahoney LJ (1922). Action currents in stomach and intestine. *Am J Physiol* **58,** 476–493.

Angeli TR, O'Grady G, Du P, Paskaranandavadivel N, Pullan AJ, Bissett IP & Cheng LK (2013*a*). Circumferential and functional re-entry of in vivo slow-wave activity in the porcine small intestine. *Neurogastroenterol Motil*; In press.

Angeli TR, O'Grady G, Paskaranandavadivel N, Erickson JC, Du P, Pullan AJ, Bissett IP & Cheng LK (2013*b*). Experimental and automated analysis techniques for high-resolution electrical mapping of small intestine slow wave activity. *J Neurogastroenterol Motil* **19,** 179–191.

Barr RC (2000). Basic Electrophysiology. In *The Biomedical Engineering Handbook: Second Edition*, ed. Bronzino JD. CRC Press LLC, Boca Raton.

Bayguinov O, Hennig GW & Sanders KM (2011). Movement based artifacts may contaminate extracellular electrical recordings from GI muscles. *Neurogastroenterol Motil* **23,** 1029–42, e498.

Berkson J, Baldes E & Alvarez WC (1932). Electromyographic studies of the gastrointestinal tract: I. The correlations between mechanical movement and changes in electrical potential during rhythmic contraction of the intestine. *Am J Physiol* **102,** 683–692.

Bortoff A (1967). Configuration of intestinal slow waves obtained by monopolar recording techniques. *Am J Physiol* **213,** 157–162.

Bozler E (1939). Electrophysiological studies on the motility of the gastrointestinal tract. *Am J Physiol* **127,** 301–307.

Bozler E (1945). The action potentials of the stomach. *Am J Physiol* **144,** 693–700.

Bueno L, Ferre JP & Ruckebusch Y (1978). Effects of anesthesia and surgical procedures on intestinal myoelectric activity in rats. *Am J Dig Dis* **23,** 690–695.

Cheng LK, O'Grady G, Du P, Egbuji JU, Windsor JA & Pullan AJ (2010). Gastrointestinal system. *WIREs Syst Biol Med* **2,** 65–79.

Cohen I & Miles R (2000). Contributions of intrinsic and synaptic activities to the generation of neuronal discharges in in vitro hippocampus. *J Physiol* **524,** 485–502.

Coronel R, De Bakker JMT, Wilms-Schopman FJG, Opthof T, Linnenbank AC, Belterman CN & Janse MJ (2006). Monophasic action potentials and activation recovery intervals as measures of ventricular action potential duration: experimental evidence to resolve some controversies. *Heart Rhythm* **3,** 1043–1050.

De-Bakker JMT & Wittkampf FHM (2010). The pathophysiologic basis of fractionated and complex electrograms and the impact of recording techniques on their detection and interpretation. *Circ Arrhythm Electrophysiol* **3,** 204–213.

Dickens EJ, Hirst GDS & Tomita T (1999). Identification of rhythmically active cells in guinea-pig stomach. *J Physiol* **514,** 515–531.

Du P, O'Grady G, Egbuji JU, Lammers WJEP, Budgett D, Nielsen P, Windsor JA, Pullan AJ & Cheng LK (2009). High-resolution mapping of in vivo gastrointestinal slow wave activity using flexible printed circuit board electrodes: methodology and validation. *Ann Biomed Eng* **37,** 839–846.

Egbuji JU, O'Grady G, Du P, Cheng LK, Lammers WJEP, Windsor JA & Pullan AJ (2010). Origin, propagation and regional characteristics of porcine gastric slow wave activity determined by high-resolution mapping. *Neurogastroenterol Motil* **22,** e292–300.

El-Sharkawy TY & Daniel EE (1975). Electrical activity of small intestinal smooth muscle and its temperature dependence. *Am J Physiol* **229,** 1268–1276.

Erickson JC, O'Grady G, Du P, Obioha C, Qiao W, Richards WO, Bradshaw LA, Pullan AJ & Cheng LK (2010). Falling-edge, variable threshold (FEVT) method for the automated detection of gastric slow wave events in high-resolution serosal electrode recordings. *Ann Biomed Eng* **38,** 1511–1529.

Franz MR (1983). Long-term recording of monophasic action potentials from human endocardium. *Am J Cardiol* **51,** 1629–1634.

Franz MR (1999). Current status of monophasic action potential recording: theories, measurements and interpretations. *Cardiovasc Res* **41,** 25–40.

Hennig GW, Costa M, Chen BN & Brookes SJ (1999). Quantitative analysis of peristalsis in the guinea-pig small intestine using spatio-temporal maps. *J Physiol* **517,** 575–590.

Hinder RA & Kelly KA (1977). Human gastric pacesetter potential. Site of origin, spread, and response to gastric transection and proximal gastric vagotomy. *Am J Surg* **133,** 29–33.

Hocke M, Schöne U, Richert H, Görnert P, Keller J, Layer P & Stallmach A (2009). Every slow-wave impulse is associated with motor activity of the human stomach. *Am J Physiol Gastrointest Liver Physiol* **296,** G709–16.

Hoffman BF, Cranefield PF, Lepeschkin E, Surawicz B & Herrlich HC (1959). Comparison of cardiac monophasic action potentials recorded by intracellular and suction electrodes. *Am J Physiol* **196,** 1297–1301.

Huang S, Nakayama S, Iino S & Tomita T (1999). Voltage sensitivity of slow wave frequency in isolated circular muscle strips from guinea pig gastric antrum. *Am J Physiol Gastrointest Liver Physiol* **276,** G518–G528.

Huh CH, Bhutani MS, Farfán EB & Bolch WE (2003). Individual variations in mucosa and total wall thickness in the stomach and rectum assessed via endoscopic ultrasound. *Physiol Meas* **24,** N15–22.

Imtiaz MS, Smith DW & Van Helden DF (2002). A theoretical model of slow wave regulation using voltage-dependent synthesis of inositol 1,4,5-trisphosphate. *Biophys J* **83,** 1877–1890.

Janssen PWM, Lentle RG, Hulls C, Ravindran V & Amerah AM (2009). Spatiotemporal mapping of the motility of the isolated chicken caecum. *J Comp Physiol B* **179,** 593–604.

Jochim K, Katz LN & Mayne W (1935). The monophasic electrogram obtained from the mammalian heart. *Am J Physiol* **111,** 177–186.

Kaiser JF (1990). On a simple algorithm to calculate the energy of the signal. In *Proc. IEEE. Int. Conf. Acoustics, Speech, Signal Processing*, pp. 381–384.

Kelly KA & Code CF (1971). Canine gastric pacemaker. *Am J Physiol* **220,** 112–118.

Lammers WJ, Al-Kais A, Singh S, Arafat K & El-Sharkawy TY (1993). Multielectrode mapping of slow-wave activity in the isolated rabbit duodenum. *J Appl Phys* **74,** 1454–1461.

Lammers WJ, Dhanasekaran S, Slack JR & Stephen B (2001). Two-dimensional high-resolution motility mapping in the isolated feline duodenum: methodology and initial results. *Neurogastroenterol Motil* **13,** 309–323.

Lammers WJEP, Stephen B & Slack JR (2002). Similarities and differences in the propagation of slow waves and peristaltic waves. *Am J Physiol Gastrointest Liver Physiol* **283,** G778–86.

Lentle RG, De Loubens C, Hulls C, Janssen PWM, Golding MD & Chambers JP (2012). A comparison of the organization of longitudinal and circular contractions during pendular and segmental activity in the duodenum of the rat and guinea pig. *Neurogastroenterol Motil* **24,** 686–e298.

Malysz J, Richardson D, Farraway L, Christen M-O & Huizinga JD (1995). Generation of slow wave type action potentials in the mouse small intestine involves a non-L-type calcium channel. *Can J Physiol Pharmacol* **73,** 1502–1511.

Marciani L (2011). Assessment of gastrointestinal motor functions by MRI: a comprehensive review. *Neurogastroenterol Motil* **23,** 399–407.

O'Grady G (2012). Gastrointestinal extracellular electrical recordings: fact or artifact? *Neurogastroenterol Motil* **24,** 1–6.

O'Grady G, Angeli TR, Du P, Lahr C, Lammers WJEP, Windsor J a, Abell TL, Farrugia G, Pullan AJ & Cheng LK (2012*a*). Abnormal initiation and conduction of slow-wave activity in gastroparesis, defined by high-resolution electrical mapping. *Gastroenterology* **143,** 589–98.e1–3.

O'Grady G, Du P, Cheng LK, Egbuji JU, Lammers WJEP, Windsor JA & Pullan AJ (2010). Origin and propagation of human gastric slow-wave activity defined by high-resolution mapping. *Am J Physiol Gastrointest Liver Physiol* **299,** G585–92.

O'Grady G, Du P, Paskaranandavadivel N, Angeli TR, Lammers WJEP, Asirvatham SJ, Windsor J a, Farrugia G, Pullan a J & Cheng LK (2012*b*). Rapid high-amplitude circumferential slow wave propagation during normal gastric pacemaking and dysrhythmias. *Neurogastroenterol Motil* **24,** e299–312.

O'Grady G, Egbuji JU, Du P, Lammers WJEP, Cheng LK, Windsor J a & Pullan a J (2011). High-resolution spatial analysis of slow wave initiation and conduction in porcine gastric dysrhythmia. *Neurogastroenterol Motil* **23,** e345–55.

O'Grady G, Pullan AJ & Cheng LK (2012*c*). The analysis of human gastric pacemaker activity. *J Physiol* **590,** 1299–1300.

Paskaranandavadivel N, Cheng LK, Du P, O'Grady G & Pullan AJ (2011). Improved signal processing techniques for the analysis of high resolution serosal slow wave activity in the stomach. *Conf Proc IEEE Eng Med Biol Soc* **1,** 1737–1740.

Paskaranandavadivel N, O'Grady G, Du P & Cheng LK (2013). Comparison of filtering methods for extracellular gastric slow wave recordings. *Neurogastroenterol Motil* **25,** 79–83.

Paskaranandavadivel N, O'Grady G, Du P, Pullan AJ & Cheng LK (2012). An improved method for the estimation and visualization of velocity fields from gastric high-resolution electrical mapping. *IEEE Trans Biomed Eng* **59,** 882–889.

Rhee P-L, Lee JY, Son HJ, Kim JJ, Rhee JC, Kim S, Koh SD, Hwang SJ, Sanders KM & Ward SM (2011). Analysis of pacemaker activity in the human stomach. *J Physiol* **589,** 6105–6118.

Richter CP (1924). Action currents from the stomach. *Am J Physiol* **67,** 612–633.

Sarna SK, Daniel EE & Kingma YJ (1971). Simulation of slow-wave electrical activity of small intestine. *Am J Physiol* **221,** 166–175.

Sarna SK, Daniel EE & Kingma YJ (1972*a*). Effects of partial cuts on gastric electrical control activity and its computer model. *Am J Physiol* **223,** 332–340.

Sarna SK, Daniel EE & Kingma YJ (1972*b*). Simulation of the electric-control activity of the stomach by an array of relaxation oscillators. *Am J Dig Dis* **17,** 299–310.

Savitzky A & Golay MJE (1964). Smoothing and differentiation of data by simplified least squares procedures. *Anal Chem* **36,** 1627–1639.

Shabetai R, Surawicz B & Hammill W (1968). Monophasic action potentials in man. *Circulation* **38,** 341–352.

Sinn DH, Min B-H, Ko E, Lee JY, Kim JJ, Rhee JC, Kim S, Ward SM & Rhee P-L (2010). Regional differences of the effects of acetylcholine in the human gastric circular muscle. *Am J Physiol Gastrointest Liver Physiol* **299,** G1198–203.

Smout AJPM, Van der Schee EJ & Grashuis JL (1980). What is measured in electrogastrography? *Digest Dis Sci* **25,** 179–187.

Spach MS, Barr RC, Serwer GA, Kootsey JM & Johnson EA (1972). Extracellular potentials related to intracellular action potentials in the dog purkinje system. *Circ Res* **30,** 505–519.

Spach MS, Miller WT, Miller-Jones E, Warren RB & Barr RC (1979). Extracellular potentials related to intracellular action potentials during impulse conduction in anisotropic canine cardiac muscle. *Circ Res* **45,** 188–204.

Suzuki N, Prosser CL & DeVos W (1986). Waxing and waning of slow waves in intestinal musculature. *Am J Physiol* **250,** G28–34.

Szurszewski JH (1998). A 100-year perspective on gastrointestinal motility. *Am J Physiol Gastrointest Liver Physiol* **274,** G447–453.

Tranquillo J V, Franz MR, Knollmann BC, Henriquez AP, Taylor D a & Henriquez CS (2004). Genesis of the monophasic action potential: role of interstitial resistance and boundary gradients. *Am J Physiol Heart Circ Physiol* **286,** H1370–81.

VanHelden DF & Imtiaz MS (2003). Ca2+ phase waves: a basis for cellular pacemaking and long-range synchronicity in the guinea-pig gastric pylorus. *J Physiol* **548,** 271–296.

Wang X-Y, Lammers WJEP, Bercik P & Huizinga JD (2005). Lack of pyloric interstitial cells of Cajal explains distinct peristaltic motor patterns in stomach and small intestine. *Am J Physiol Gastrointest Liver Physiol* **289,** G539–49.

Xue S, Valdez DT, Tremblay L, Collman PI & Diamant NE (1995). Electrical slow wave activity of the cat stomach: its frequency gradient and the effect of indomethacin. *Neurogastroenterol Motil* **7,** 157–167.

Yassi R, O'Grady G, Paskaranandavadivel N, Du P, Angeli TR, Pullan AJ, Cheng LK & Erickson JC (2012). The gastrointestinal electrical mapping suite (GEMS): software for analyzing and visualizing high-resolution (multi-electrode) recordings in spatiotemporal detail. *BMC Gastroenterol* **12,** 60.

Yin J & Chen JDZ (2013). Electrogastrography: methodology, validation and applications. *J Neurogastroenterol Motil* **19,** 5–17.

Yue AM, Paisey JR, Robinson S, Betts TR, Roberts PR & Morgan JM (2004). Determination of human ventricular repolarization by noncontact mapping: validation with monophasic action potential recordings. *Circulation* **110,** 1343–1350.

Tables and Figures

Table 1

	Pre-nifedipine	**Post-nifedipine**	**Significance**
Velocity (mm s^{-1})	12.8 ± 1.1	11.9 ± 0.8	$p = 0.55$
Downstroke Width (s)	0.4 ± 0.05	0.4 ± 0.04	$p = 0.96$
Downstroke Rate (μV s^{-1})	-123.0 ± 20.7	-94.2 ± 11.5	$p = 0.22$
Amplitude (μV)	41.7 ± 5.8	29.1 ± 4.2	$p = 0.10$
Frequency (cpm)	15.6 ± 1.3	11.8 ± 0.8	$p = 0.03$

Table 1: Comparison of average slow wave characteristics before and after the administration of nifedipine. Slow wave velocity, downstroke width, downstroke rate, and amplitude all remained similar before and after nifedipine was administered. Slow wave frequency decreased by 24%.

Table 2

	Suction	**Conventional**	**Significance**
Morphology	Monophasic	Biphasic	-
Downstroke Rate ($\mu V\ s^{-1}$)	-1000 ± 460	1120 ± 490	$p < 0.0001$
Amplitude (μV)	652 ± 178	399 ± 144	$p < 0.0001$
Frequency (cpm)	3.6 ± 0.3	3.6 ± 0.2	$p = 0.99$
Activation-Recovery Interval (s)	6.2 ± 0.4	6.1 ± 0.5	$p = 0.15$

Table 2: Slow wave extracellular potential characteristics for suction and conventional extracellular methods. Morphology features differed, but frequency and activation-recovery interval were highly consistent between the two recording methods.

Figure 1

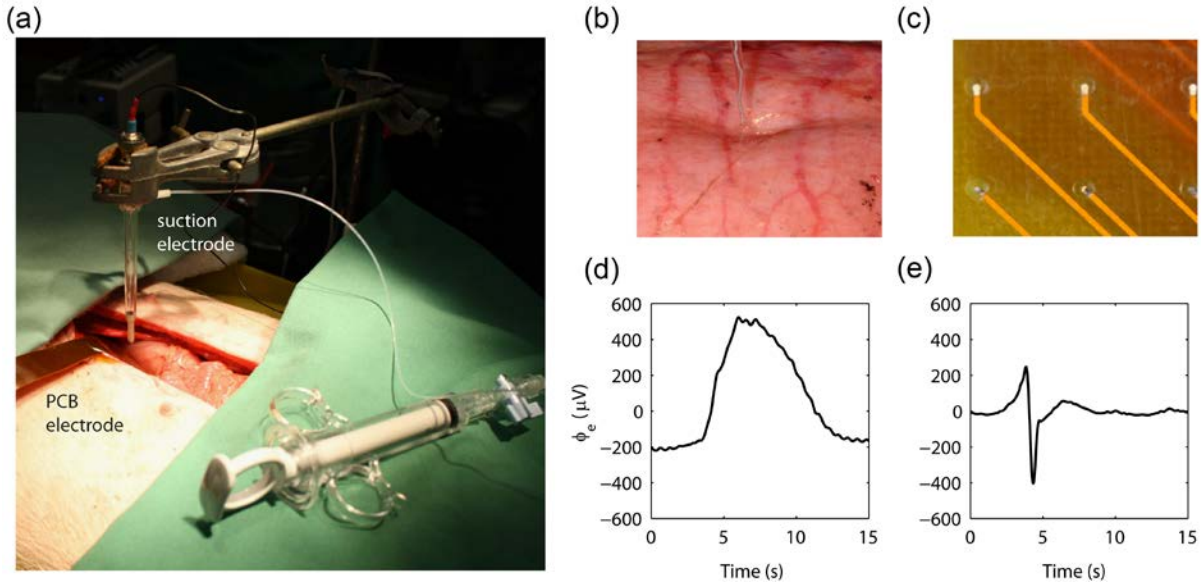

Figure 1: Extracellular slow wave recording modalities. **(a)** A suction electrode and conventional serosal contact electrodes were employed simultaneously *in-vivo* on adjacent sections of the gastric serosa. **(b)** The tip of the capillary of the suction electrode was indented slightly into the gastric serosa. **(c)** The conventional serosal contact electrodes were placed directly on the serosa, and held in contact with gentle overlying pressure using soaked gauze. **(d, e)** Experimental recordings of slow waves recorded by the conventional serosal contact (d) and suction electrode (e) are shown.

Figure 2

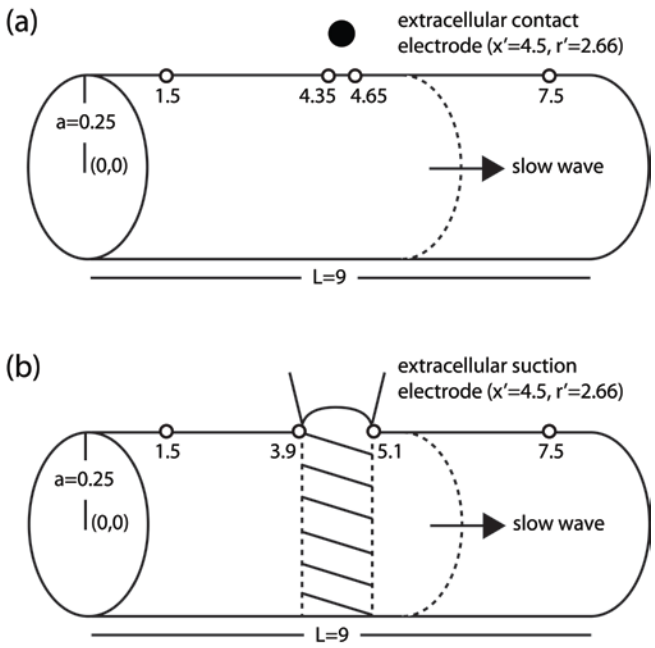

Figure 2: Schematic models of **(a)** conventional serosal contact electrode and **(b)** suction electrode recordings. All values shown are in mm. Electrode position and fibre radius and length were identical for each electrode type. Signals were evaluated at four locations: at 3 mm in each direction from the centre of the electrode (*x* = 1.5 and 7.5 mm), and at each edge of the electrode (*x* dependent on electrode contact diameter, with values as shown).

Figure 3

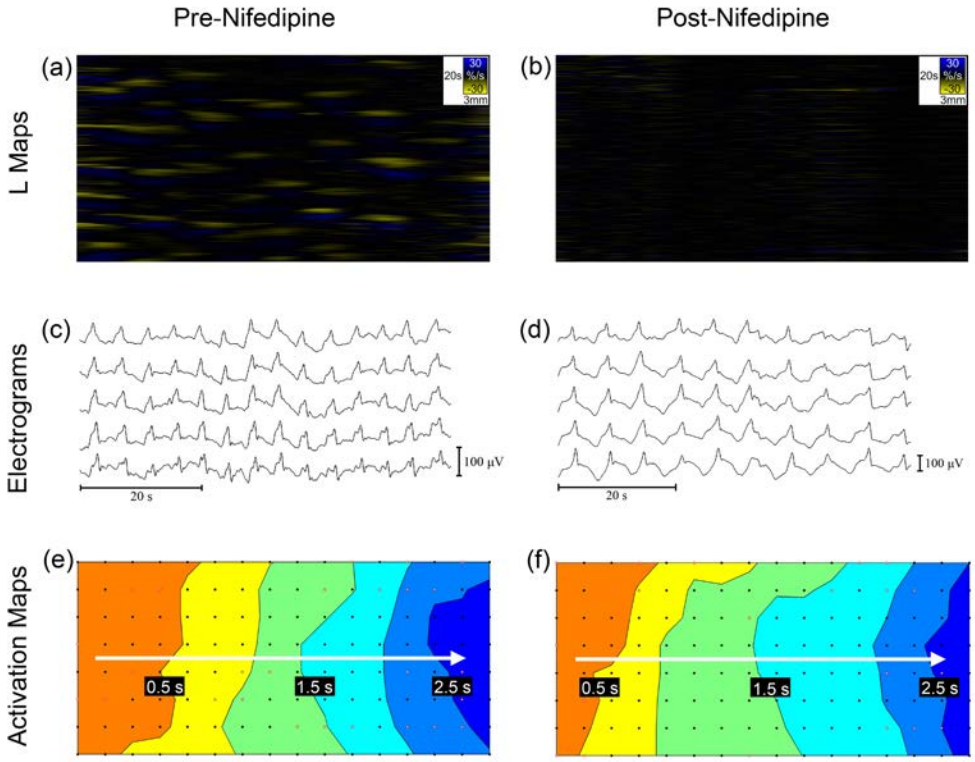

Figure 3: Comparison of intestinal slow wave potentials before and after nifedipine administration. L-maps of video analysis are shown in (a, b); yellow bands show contraction and blue bands show relaxation. **(a)** Contractile activity was evident in 4/5 pigs before nifedipine was administered. In this recording, widespread segmental contractions occurred at a frequency of 2.3 cpm. **(b)** Nifedipine abolished detectable motion in all experiments, with only random background noise observed. This recordings is from the same intestinal segment as (a), after nifedipine was administered. **(c, d)** Electrograms. Slow waves were observed in all recordings before and after the application of nifedipine, with representative signals shown. Full quantification of slow wave characteristics is reported in Table 1. **(e, f)** Activation maps showing the propagation of a single slow wave in time, from orange (early) to blue (late). Slow wave propagation patterns remained similar before and after the administration of nifedipine. Activation maps are presented with 0.5 s isochronal intervals.

Figure 4

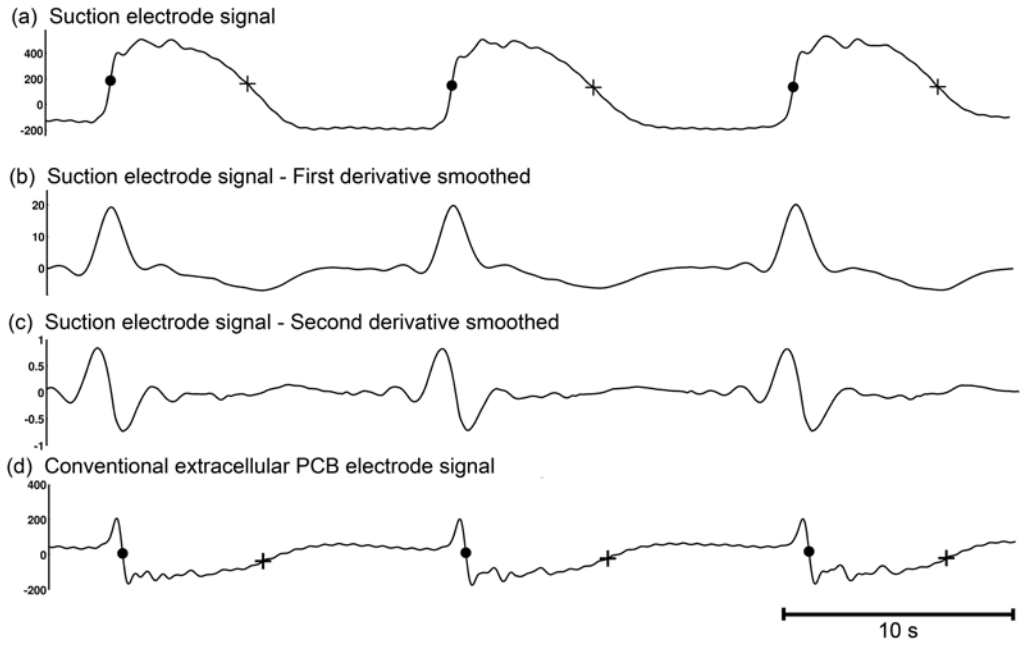

Figure 4: Gastric extracellular slow wave potentials. **(a)** A monophasic electrode signal recorded experimentally by the suction electrode (Figure 1a) with activation and recovery times marked by a dot and '+', respectively. **(b, c)** The first and second derivative of the monophasic suction electrode signal of the monophasic suction electrode signal. **(d)** The biphasic electrode signal was recorded experimentally by a conventional serosal contact electrode (Figure 1b) with the activation and recovery times marked by a dot and '+', respectively. The activation-recovery interval was consistent between the biphasic and monophasic waveforms (refer Table 2). The biphasic signal demonstrated a morphology that was consistent with the smoothed second derivative of the monophasic suction electrode (c).

Figure 5

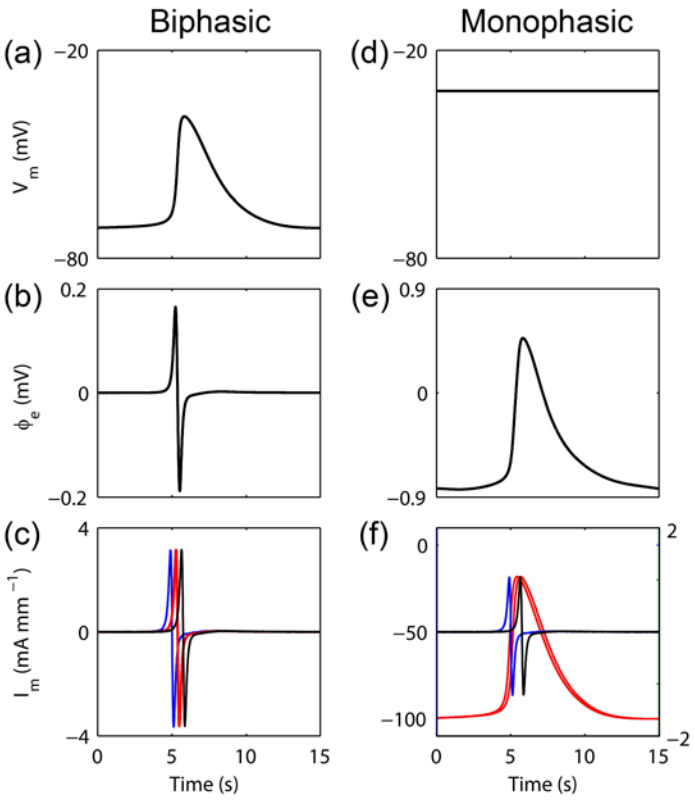

Figure 5: Gastric slow wave extracellular potentials simulated in the model outlined in Figure 2. Left column: biphasic potential (conventional serosal contact electrode); right column: monophasic potential (suction electrode). **(a)** Simulated membrane potential sampled at *x* = 4.5 mm along the fibre; **(b)** simulated extracellular potential at 2.66 mm away from the fibre; **(c)** I_m sampled at four points at *x* = 1.5 (blue), 4.35 (red), 4.65 (red), and 7.5 mm (black). The two traces shown in red are nearest to the electrode and are nearly identical in time. **(d)** simulated membrane potential sampled at x = 4.5 mm along the fibre. To simulate suction pressure, the membrane potential was held at -32 mV; **(e)** simulated extracellular potential; **(f)** I_m sampled at four points at *x* = 1.5 (blue), 3.9 (red), 5.1 (red), and 7.5 mm (black). The two traces shown in red are nearest to the electrode and are nearly identical in time. The left axis correlates to the monophasic red traces, and the right axis correlates to the biphasic blue and black traces. The morphologies of the modelled biphasic and monophasic

potentials were concordant with the experimental data obtained using these techniques (Figures 1, 4).